An Eco-friendly Fabrication of Silver Chloride Nanoparticles (AgCLNPs) using Onopordum acanthium L extract Induces Apoptosis in Breast Cancer MDA-MB-232 Cells

Seyedeh Negin Shahcheraghi
Islamic Azad University Central Tehran Branch
Seyed Ataollah Sadat Shandiz (ata.sadatshandiz@iauctb.ac.ir)
Islamic Azad University
Bahareh Pakpour
Islamic Azad University Central Tehran Branch

Research Article

Keywords: MDA_MB232 cells, silver chloride nanoparticles, Apoptosis, cytotoxicity.

Posted Date: March 19th, 2021

DOI: https://doi.org/10.21203/rs.3.rs-303501/v1

Abstract

In the current experimental work, silver chloride nanoparticles (AgClNPs) were fabricated using *Onopordum acanthium* L extract and their apoptotic and cytotoxicity properties on breast cancer MDA_MB232 and normal HEK293 cell lines were also evaluated. AgClNPs formation was determined by X-ray diffraction (XRD), scanning electron microscopy (SEM), and energy dispersive spectroscopy (EDS) profile. Effect of fabricated AgClNPs on MDA_MB232 and HEK293 cells viability was performed using colorimetric MTT assay. Alterations in the mRNA expression levels of *CAD* and *Bax* genes in MDA-MB-232 cells were done using quantitative real-time reverse transcription-PCR (qRT-PCR) method. Subsequently, apoptotic properties were determined using flow cytometry and fluorescence microscopy studies. MTT results investigated that AgCLNPs have a significant dose-dependent lethal activity on MDA_MB232 compared to HEK293 cell lines. Quantitative real-time reverse transcription-PCR (qRT-PCR) results have also shown that AgCLNPs could up-regulate the apoptotic *Bax* and *CAD* gene expressions in the MDA_MB232 cells. Additionally, apoptotic assessment was performed by cell cycle analysis, annexin V/PI test, Hoescht 33258 dye, acridine orange and ethidium bromide (AO/EB) staining along with the detection of the reactive oxygen species (ROS) generation. Our results suggest that novel silver chloride nanoparticles fabricated by *Onopordum acanthium* L extract can display some promising cytotoxic properties through inducing apoptosis pathway.

Introduction

Nanotechnology, including the production and use of nanoparticle materials, is rapidly growing, which has a wide range of applications in various scientific and industrial fields (Reddy et al. 2014). Advances in nanotechnology and an in-depth understanding of cellular processes have helped researchers in designing and synthesizing nanoparticles for therapeutic and diagnostic purposes (Umar et al. 2019). It should be noted that different preparation methods cause different structural properties in the synthesized nanoparticles, which in turn lead to different functional properties in nanoparticles (Rajeshkumar et al. 2018). Nanoparticles due to their wide applications in industry, medicine, and biotechnology, have attracted many scientists' attention. Among these, silver nanoparticles (AgNPs) and silver chloride nanoparticles (AgCLNPs) were found as more effective products due to their promising biomedical applications (Dhas et al. 2014).

Currently, many approaches have been developed for the fabrication of metallic nanoparticles using physical, chemical, and biological methods (Chugh et al. 2018). Biological procedure of synthesis includes plants or the green synthesis that is well-known due to their simplicity, cost- effectiveness, biocompatibility, and feasibility for nanoparticle fabrication over the chemical and physical methods (Singh et al. 2018). Moreover, the green synthesis of nanoparticles from plant extracts is the greatest ideal strategy for cancer treatment due to its environmentally friendly approach (Popescu et al. 2010). Traditionally, *Onopordum acanthium* L., called as Scotch thistle, is a widely distributed plant used in medical field. Additionally, *Onopordum acanthium* L displayed different *in vitro* and *in vivo* pharmacological properties such as Antipyretic, Antihypertensive, anti-inflammatory, Antibacterial, and

Antiradical (Garsiya et al. 2019). Thus, the phytochemicals of *Onopordum acanthium* L can act as a reducing and stabilizing agent in the preparation of green AgNPs, which can consequently lead to the enhanced cytotoxicity activity.

Previous studies implicated that green-route mediated fabrication of AgNPs inhibits the progression of tumor cell lines in experimental animals (Murugesan et al. 2019; Jeyaraj et al. 2013). The biologically fabricated AgNPs inhibit the A549 lung cancer cells by the caspase-dependent mitochondrial pathway (Kanipandian et al. 2019). George et al. in their study investigated the cytotoxicity of biosynthesized AgNPs, and showed that it is associated with the nuclear damage, dysfunction of cellular mitochondrial membrane, and intracellular reactive oxygen species (ROS) production for human breast cancer cells MCF-7 (George et al. 2018).

However, a limited number of investigations have been performed on the cytotoxic effect of silver chloride nanoparticles on breast cancer cell lines, so in this study, we aimed to investigate it. According to a previous research, the biosynthesis of AgClNPs using *Onopordum acanthium* L extract has not been reported. In our work, we investigated the simple and rapid biosynthesis of silver chloride nanoparticles using the *Onopordum acanthium* L extract, as well as its apoptotic effects on breast cancer MDA-MB232 and normal HEK-293 cell lines.

Materials And Methods

Preparation of green AgCLNP

At first, to prepare the hydroalcoholic extract of plant, we added 50 grams of powdered dried plant *Onopordum acanthium* L into 200 cc of 50% ethanol, followed by centrifugation at 14000 rpm for 20 minutes. The obtained solution was then passed through a filter paper, dried, and stored in the refrigerator for further testing. For nanoparticles' fabrication, the first 100 mL of a solution of 1 mM silver chloride was prepared in distilled water. Thereafter, 5 ml of 4 mg/mL solution of *Onopordum acanthium* extract and 1 mM KCL salt were drop wise added to the stirred silver nitrate $AgNO_3$ solution. Next, the resulted solution was stirred for 24 hours at room temperature. This solution was then centrifuged at 13,000 rpm for 10 minutes; the supernatant was discarded and then centrifuged again with distilled water. To investigate the purification of silver chloride nanoparticles, the remained pellets were dissolved in 500 ml of deionized water, incubated it for 1 minute, and then centrifuged for 10 minutes at 3000 rpm.

The fabrication of AgClNPs was monitored by the calculation of the phase identification using X-ray diffraction (XRD) technique. The size and surface morphological properties of the synthesized AgClNPs were investigated using FESEM image by utilizing the Philips XL30 instrument. Moreover, the chemical composition elements of AgClNPs were identified by the energy-dispersive spectroscopy (EDS) analysis.

Cell culture

The MDA-MB232 and HEK293 cell lines were cultured in $RPMI_{1640}$ medium with 10% FBS serum and 1% streptomycin- penicillin solution. The cells were then stored at 37 ° C in an about 70% humid atmosphere with a concentration of 5% CO_2.

Cell viability assay

To exhibit the *in vitro* cytotoxicity, the colorimetric MTT method was employed for investigating the lethal properties of silver chloride nanoparticles. Afterward, different concentrations (0, 0.3125, 0.625, 12.5, 25, 50, and 100mg/mL) of AgClNPs were added to the cells (1×10^4 cell /well) seeded on 96-well plate, which were incubated overnight. Thereafter, 100 µl of 0.05mg/well MTT solution was added to the plate at 37˚C. To solubilize the viable cells formazan crystals production, we added 100 µl/well of dimethyl sulfoxide (DMSO) to them. Finally, the optical density of the measurement was evaluated at 570 nm.

Real time PCR reaction analysis

To evaluate the qRT-PCR method, total RNA extraction was performed using the RNA extraction kit in terms of the manufacturer's protocols (Qiagen, Valencia, CA). PrimeScript™ RT Kit (Takara, Japan) was utilized for the fabrication of complementary DNA (cDNA). Briefly, 100 ng cDNA (1 micro Liter) was used for real time PCR reaction, followed by the addition of 10 µL of SYBR green master mix in a total volume of 20 µl per reaction. *Bax* and *CAD* primers were then developed using NCBI primer blast in this study (Table 1). Thereafter, qRT-PCR was performed for 10 min at 95°C as an initial denaturation and 40 cycles for 15 s at 95°C were also done, followed by annealing for 1 min at 60°C. Additionally, the result was evaluated by ABI StepOne using the Applied Biosystems qRT-PCR thermo cycler device.

Fluorescence microscopy study

The apoptotic and necrotic patterns in cells after the treatment of AgClNPs were ascertained using a dual acridine orange and ethidium bromide (AO/EB) staining. The MDA-MB232 cells were exposed to nanoparticles, fixed by the addition of 4% formaldehyde, and AO/EB solution (10 µL), followed by 5 min incubation. For Hoechst nuclear staining, the cells were exposed to AgClNPs and then washed with PBS. A Hoechst 33258 solution was added for 5 min in the dark followed by washing thrice with PBS. The cells were finally visualized by fluorescence microscope.

Annexin V/PI staining by flow cytometery

Apoptotic and necrotic percentages were assessed using the fluorescein isothiocyanate (FITC)-Annexin-V/PI staining kit (Roch, Switzerland). Subsequently, the MDA-MB232 cells, at a density of 3×10^5 cells per well, were allowed to be treated by 58.61 mg/mL of AgClNPs. After the incubation for 24 h, the cells were washed, followed by re-suspending in binding buffer, and staining with in Annexin V/PI in terms of the kit's Protocol, which were then acquired using a flow cytometer.

Detection of reactive oxygen species

To assess the effect of the produced AgClNPs on intracellular reactive oxygen species (ROS) generation, 2',7'-dichloro dihydro fluorescein diacetate (DCFH-DA) assay was evaluated by flow cytometry. Firstly, MDA-MB232 cells were seeded in 6-well plates, which were then allowed to grow overnight in the CO_2 incubator. For ROS activity, the cells were washed with PBS and 20 µM of DCFH-DA dye was pretreated for 30 min followed by employing flow cytometry.

Cell cycle evaluation

The cell cycle assay was further done via flow cytometry for the determination of the properties of AgClNPs on cell cycle distribution for 24 h. Afterward, the MDA-MB232 cells were treated with 58.61 mg/mL of the AgClNPs and were then washed, collected, and fixed in cold ice 70% ethanol. The cells were washed again, followed by staining with PI and 100 µg/ml of RNase treatment for 1 hour at 25°C. Finally, the cell DNA content was monitored the cell cycle distribution using flow cytometer.

Results And Discussion

Synthesis of AgClNPs

The application of nanomaterials in biomedical has been growing in recent years (Greque de Morais et al. 2014). Many research groups reported the roles of different metal nanoparticles such as cancer therapy, molecular imaging, hyperthermal therapy, and drug delivery properties in this field (Mukherjee et al. 2020; Chenthamara et al. 2019).

Previous investigations revealed the anticancer properties exhibited by this plant as well as bacterial-derived nanoparticles.

The bio-fabrication of AgClNPs using cell-free supernatant of *Escherichia coli* culture has been reported by Bigdeli et al. (Bigdeli et al. 2019). They investigated the anti-cancer properties of AgClNPs in human MCF-7 breast cancer cells. In our work, for the first time, the anti-cancer properties of AgCLNPs fabricated by the *Onopordum acanthium* extract were confirmed. This plant-mediated green route was found to be cost-effective, fast, simple, and non-toxic for environment (Salem et al 2020). Different studies have also investigated that the *Onopordum acanthium* L are rich in different chemical agents such as Lignans (Lajter et al. 2015), Flavonoids (Habibatni et al. 2017), Coumarins (Bogs et al. 1965), Terpenoids (Ivanova et al. 2010), Tocols, and Steroids (Zhelev et al. 2014), so it has been employed in traditional medicine as a cardiotonic and antitumor agent. Fabrication of *Onopordum acanthium* extract-mediated AgCLNPs was characterized by a change in the mixture from colorless to purple color.

In our study, the silver and chloride were the maximum constituent elements in the fabricated AgClNPs as observed by EDS profile. According to figure 1, further peaks such as Silisium, Aluminium, Magnesium, Cupper, and Carbon ascertain the existence of compounds, which are biomolecules attached to the NPs.

The XRD pattern's analysis was performed to describe the crystalline nature of AgClNPs according to the cubic structure (FCC) (Figure 2). Notably, the identification of AgClNPs was consistent with the Joint Committee on Powder Diffusion Standards (JCPDS) database (file no. 85–1355).

The morphological determination of nanoparticles was established by SEM image. The fabricated AgClNPs appear to have spherical nature with a particle diameter ranged from 92.53 to 157.7 nm (Figure 3).

Evaluation of cell viability assay

To determine the effect of IC_{50} dose of nanoparticles on cell lines, we examined MDA_MB232 and HEK293 cells treated with 0.3125, 0.625, 12.5, 25, 50, and 100mg/mL of AgClNPs for overnight using MTT assay. In this regard, AgClNPs were able to decrease cell viability in a dose-dependent manner, as shown in Figure 4. Moreover, IC_{50} concentration of AgClNPs toward MDA-MB232 and HEK293 cells was 58.61 and 139.6 µg/mL, respectively.

Different types of reports are available on anti-tumor effect of green silver nanoparticles toward various cell lines such as MCF-7, A549 (Venugopal et al. 2017), PC-3 (He et al. 2016), and HTC-116 cells (Kuppusamy et al. 2016). AgNPs fabricated using the culture supernatant of *Bacillus funiculus* showed the reduced cell viability against MDA-MB-231 breast cancer cells using 10 µg/mL and higher amounts (Gurunathan et al. 2013).

However, a limited number of investigations have showen the cytotoxicity effect of the biologically fabricated silver chloride nanoparticles toward cell lines *in vitro*. Sattari et al. (2020) using *Levisticum Officinale* extract, reported that Ag and Ag chloride nanoparticles were toxic to MDA-MB-468 breast cancer cells (Sattari et al. 2020). Moreover, charelli et al. (2018) in their study revealed that silver chloride nanoparticles from *B. megaterium* have a little effect on toxicity of human adipose tissue stem cells (ASCs) in spheroid 3D culture. Furthermore, they showed that sub-lethal AgCLNP doses trigger the ROS production at day 7 after the exposure (Charelli et al. 2018).

Estimation of AgClNP apoptotic properties

To further examine the effect of AgCLNP on cell cycle phase's distribution, flow cytometry methods were performed. Therefore, cell cycle progression was arrested in MDA_MB232 cells, followed by the treatment with AgClNP.

In addition, Ag nanoparticles mediated cell cycle arrest in all phases. Interestingly, a previously performed investigation in Ehrlich ascites carcinoma (EAC) cells *in vivo* and human glioblastoma stem cells (GSCs) *in vitro* found that silver/silver chloride nanoparticles fabricated from *Kaempferia rotunda* fruit extract increased the population of cells in the G2/M phase. Accordingly, the increase in IL1, p21, TNFa, TLR9, IKK, and NFκB genes' expressions were also observed that were related to apoptosis in GSCs (Kabir et al. 2020). Another investigation showed that the AgNPs-mediated extract of *Nepeta deflersiana* plant up-

regulated the ROS and lipid peroxidation (LPO) in cervical cancer cells (HeLa), which consequently caused an increase in apoptotic SubG1 peak (Al-Sheddi et al. 2018). The triggering apoptosis due to the existence of SubG1 peak in the process of cell cycle confirmed the involvement of apoptotic cell death pathway (Pumiputavon et al. 2017). According to cell cycle analysis, an increase was observed in the number of cell population in sub-G1 phase (implicates apoptotic pathway cell death) compared to the control cells (Figure 5).

Notably, several investigations were conducted on the potentials of different nanoparticles in cell's ROS production. ROS in tumoral cells can act in the regulation of energy metabolism, cell growth, motility, autophagy, and cell death (Liou et al. 2010).

The production of ROS induced by nanoparticles lead to lipid peroxidation, nucleic acid cleavage, biomolecules' destruction, membrane and organelle structures' destruction, and mitochondrial membrane potentials (MMP) increase, which further resulted in apoptosis and necrosis (Yu et al. 2020).

Mao et al. suggested that lethal and sublethal doses of the fabricated citrate-coated AgNPs can induce ROS-mediated stress responses such as DNA damage, apoptosis, and autophagy on *in vivo* platform *Drosophila melanogaster* (Mao et al. 2018). Similar investigations performed on the activity of the biologically synthesiszed Ag/AgCl NPs by leafy vegetable of *Rumex. acetosa* demonstrated high antioxidant and cytotoxicity activities against the human osteosarcoma (HOS) cell lines (Kota et al. 2017).

In this regard, ROS levels induced by AgClNP were validated using flow cytometric analysis. Importantly, flow cytometric analysis followed by staining with DCFH-DA dye was done to explain the role of oxidative stress in nanoparticles-treated cell-death. The results reveal that AgClNPs has significantly increased ROS levels in MDA_MB232 cells compared to those untreated cells (Figure 6). These results suggest that ROS productions in MDA-MB-232 cells play significant roles in triggering cells death.

Alterations in the mRNA expression levels of *CAD* and *Bax* genes in MDA-MB-232 cells were done using qRT-PCR method followed by the exposure to nanoparticle (as shown in Figure 7). Furthermore, the Caspase-activated DNase (*CAD*) and *Bax* genes were shown to be involved in the apoptosis pathway. The *Bax* gene is known as pro-apoptotic member of the B cell lymphoma-2 (*Bcl-2*) gene family, which is the main regulator of this pathway. Thus, the dysfunction in *Bcl-2* gene family activities has been associated with many diseases (Siddiqui et al. 2015).

Within the activation of apoptosis pathway, DNA fragmentation has occurred, which is responsible for triggering apoptotic bodies. The Caspase-activated DNase (CAD), as a nuclease enzyme, cleaves dsDNA, which helps chromatin condensation and apoptotic DNA fragmentation (Miles et al. 2017).

Bigdeli et al. have reported that AgClNPs-mediated apoptosis is dependent on the increased *p53, bax, caspase 3, caspase 8,* and *caspase 9* genes' expressions (Bigdeli et al. 2019). According to our study, the results of real time PCR displayed that the expression of *CAD* was up-regulated by a 5.5-fold, while mRNA

level of *Bax* was down-regulated by 0.53-fold when compared to the untreated cells, proposing that AgClNPs trigger apoptosis via an intrinsic (mitochondrial mediated) pathway.

To determine the mechanism of cell death in the cancer cells, annexin V/PI flow cytometry was employed. In the treatment of MDA-MB-232 cells by IC_{50} of AgClNPs (58.61 g/mL), 35.5%, and, 2.89% of early and late stages' apoptosis were observed, respectively (Figure 8). While the untreated cells revealed 0.3% and 0.1 % of early and late stages' apoptosis, respectively.

Considering that the apoptosis/necrosis induction causes change in cell's morphology, we explored AO/EB double staining to discriminate the apoptotic, necrotic pathway, and integrity of membrane in MDA-MB-232 cells after the exposure to nanoparticles overnight. The Hoescht 33258 results reveal that AgClNPs has increased apoptosis through nuclear fragmentation, cytoplasmic and chromatin condensation (Figure9). Chromatin condensation, nuclear fragmentation, cell membrane blebbing, and cell shrinkage are usual apoptotic properties (Curčić et al. 2012).

Viable cells with intact DNA display a green color in their nuclei. Apoptotic cells with the condensed DNA show orange nuclei, while red nuclei represent necrotic cells. According to findings shown in Figure 10 the increased number of apoptotic cells can be observed in comparison with untreated cells, confirming flow cytometric results.

Conclusion

In summary, AgClNPs were fabricated from the *Onopordum acanthium* extract, which were confirmed by XRD, SEM, and EDS profile. Anti-cancer properties of *Onopordum acanthium* extract-mediated AgClNPs are due to the increased ROS level, decreased cell viability, modulation of pro-apoptotic *Bax* gene, sub-G1 cell cycle arrest, and the inhibited cell growth significantly due to the apoptosis of MDA-MB232 cells. For the breast cancer therapy, further *in vivo* studies are required to understand the efficacy of the *Onopordum acanthium* extract-mediated AgClNPs.

Declarations

Author contributions

Conceptualization: SAS, SNS, and BP; methodology: SAS, SNS, and BP; validation: SAS, SNS; formal analysis: SAS, SNS, and BP; investigation: SAS, SNS, and BP; data curation: BP; writing—original draft preparation: SAS; writing—review and editing: SAS; visualization: SAS, SNS, and BP; supervision: SAS; project administration: SAS.

Funding

There is no funding in this work

Data availability

Not applicable.

Declarations

Ethics approval and consent to participate

This article has not been report on or involves the use of any animal model. All participants have been agreed that this work will be published.

Consent for publication

Not applicable.

Competing interests

All of the authors declare that there are no competing interests.

References

Al-Sheddi ES, Farshori NN, Al-Oqail MM, Al-Massarani SM, Saquib Q, Wahab R, Musarrat J, Al-Khedhairy AA, Siddiqui MA (2018) Anticancer Potential of Green Synthesized Silver Nanoparticles Using Extract of *Nepeta deflersiana* against Human Cervical Cancer Cells (HeLA). Bioinorg Chem Appl 2018:9390784.

Bigdeli R, Shahnazari M, Panahnejad E, Ahangari Cohan R, Dashbolaghi A, Asgary V (2019) Cytotoxic and apoptotic properties of silver chloride nanoparticles synthesized using *Escherichia coli* cell-free supernatant on human breast cancer MCF 7 cell line. Artif Cells Nanomed Biotechnol 47:1603–1609.

Bogs HU, Bogs U (1965) Constituents of *Onopordum acanthium*. L. Coumarins and flavones. Pharmazie 20: 706–709.

Charelli LE, Muller N, Silva KR, Lima LMTR, Anna CS, Baptista LS (2018) Biologically produced silver chloride nanoparticles from *B. megaterium* modulate interleukin secretion by human adipose stem cell spheroids, Cytotechnology 70:1655–1669.

Chenthamara D, Subramaniam S, Ramakrishnan SG, *et al*. (2019) Therapeutic efficacy of nanoparticles and routes of administration. Biomater Res 23. https://doi.org/10.1186/s40824-019-0166-x.

Chugh H, Sood D, Chandra I, Tomar V, Dhawan G, Chandra R (2018) Role of gold and silver nanoparticles in cancer nano-medicine. Artif Cells, Nanomed Biotechnol 46:1210-1220.

Curčić MG, Stanković MS, Mrkalić EM, Matović ZD, Banković DD, Cvetković DM, Dačić DS, Marković SD (2012) Antiproliferative and proapoptotic activities of methanolic extracts from *ligustrum vulgare* L. as an individual treatment and in combination with palladium complex. Int J Mol Sci 13: 2521–2534.

Dhas TS, Ganesh Kumar V, Karthick V, Angel KJ, Govindaraju K (2014) Facile synthesis of silver chloride nanoparticles using marine alga and its antibacterial efficacy. Spectrochimica Acta Part A: Mol Biomol Spectroscopy 120: 416–420.

Garsiya ER, Konovalov DA, Shamilov AA, Glushko MP, Orynbasarova KK (2019) A Traditional Medicine Plant, *Onopordum acanthium* L. (Asteraceae): Chemical Composition and Pharmacol Res, Plants (Basel) 8:40.

Greque de Morais M, Martins VG, Steffens D, Pranke P, Vieira da Costa JA, (2014) Biological Applications of Nanobiotechnology. J Nanosci Nanotechnol 14:1007–1017.

Gholami N, Ahangari Cohan R, Razavi A, Bigdeli R, Dashbolaghi A, Asgary V (2020) Cytotoxic and apoptotic properties of a novel nano-toxin formulation based on biologically synthesized silver nanoparticle loaded with recombinant truncated pseudomonas exotoxin A, J Cellular Physiol 235: 3711-3720.

Habibatni S, Zohra AF, Khalida H, Anwar S, Mansi I, Awadh Ali NA (2017) *In-vitro* antioxidant, Xanthine oxidase-inhibitory and *in-vivo* Anti-inflammatory, analgesic, antipyretic activity of *Onopordum acanthium*. Int J Phytomed 9: 92–100.

He Y, Du Z, Ma S, Cheng S, Jiang S, Liu Y, Li D, Huang H, Zhang K, Zheng X (2016) Biosynthesis, antibacterial activity and anticancer effects against prostate cancer (PC-3) cells of silver nanoparticles using *Dimocarpus Longan* Lour. Nanoscale Res Lett 11: 300.

Ivanova LR, Butenko LI, Ligai LV, Sbezhneva VG (2010) Determination of iridoids in the herb of *Onopordum acanthium*, genus Onopordum. Chem Plant Mater 4:131–133.

George BPA, Kumar N, Abrahamse H, *et al*, (2018) Apoptotic efficacy of multifaceted biosynthesized silver nanoparticles on human adenocarcinoma cells. Sci Rep 8: 14368.

Gurunathan S, Han JW, Eppakayala V, Jeyaraj M, Kim JH (2013) Cytotoxicity of Biologically Synthesized Silver Nanoparticles in MDA-MB-231 Human Breast Cancer Cells. BioMed Res Int ID 535796. https://doi.org/10.1155/2013/535796.

Jeyaraj M, Sathishkumar G, Sivanandhan G, *et al* (2013) Biogenic silver nanoparticles for cancer treatment: an experimental report. Colloids Surf B Biointerfaces 106: 86–92.

Kabir SR, Dai Z, Nurujjaman M, Cui X., Asaduzzaman AKM, Sun B, Zhang X, Dai H, Zhao X (2020) Biogenic silver/silver chloride nanoparticles inhibit human glioblastoma stem cells growth *in vitro* and Ehrlich ascites carcinoma cell growth *in vivo*. J Cell Mol Med;00:1–12. DOI: 10.1111/jcmm.15934.

Kanipandian N, Li D, Kannan S (2019) Induction of intrinsic apoptotic signaling pathway in A549 lung cancer cells using silver nanoparticles from *Gossypium hirsutum* and evaluation of *in vivo* toxicity. Biotechnol Rep23. https://doi.org/10.1016/j.btre.2019.e00339.

Kota S, Dumpala P, Anantha RK, Verma MK, Kandepu S (2017) Evaluation of therapeutic potential of the silver/silver chloride nanoparticles synthesized with the aqueous leaf extract of *Rumex acetosa.* Sci Rep 7:11566.

Kuppusamy P, Ichwan SJ, Al-Zikri PNH, Suriyah WH, Soundharrajan I, Govindan N, Maniam GP, Yusoff MM (2016) *In vitro* anticancer activity of Au, Ag nanoparticles synthesized using *Commelina nudiflora* L. aqueous extract against HCT-116 colon cancer cells. Biol Trace Elem Res 173: 297–305.

Lajter I, Pan SP, Nikles S, Ortmann S, Vasas A, Csupor-Löffler B, Forgó P, Hohmann J, Bauer R (2015) Inhibition of COX-2 and NF-κB1 Gene Expression, NO Production, 5-LOX, and COX-1 and COX-2 Enzymes by Extracts and Constituents of *Onopordum acanthium*. Planta Med 81:1270–1276.

Liou GY, Storz P (2010) Reactive oxygen species in cancer. Free Radic Res 44 doi:10.3109/10715761003667554.

Mao BH, Chen ZY, Wang YJ, Yan SJ (2018) Silver nanoparticles have lethal and sublethal adverse effects on development and longevity by inducing ROS-mediated stress responses, Sci Rep 8: 2445.

Mukherjee S, Liang L, Veiseh O (2020) Recent Advancements of Magnetic Nanomaterials in Cancer Therapy. Pharmaceutics 12:147. doi:10.3390/pharmaceutics12020147.

Murugesan K, Koroth J, Srinivasan PP, Singh A, Mukundan S, Karki SS, Choudhary B, Gupta CM (2019) Effects of green synthesised silver nanoparticles (ST06-AgNPs) using curcumin derivative (ST06) on human cervical cancer cells (HeLa) *in vitro* and EAC tumor bearing mice models. Int J Nanomed 14:5257—5270.

Miles M, Hawkins C (2017) Executioner caspases and CAD are essential for mutagenesis induced by TRAIL or vincristine. Cell Death Dis 8 https://doi.org/10.1038/cddis.2017.454.

Popescu M, Velea A, Lorinczi A (2010) Biogenic production of nanoparticles, Dig J Nanomater Bios 5: 1035–1040.

Pumiputavon K, Chaowasku T, Saenjum C, *et al*. (2017) Cell cycle arrest and apoptosis induction by methanolic leaves extracts of four Annonaceae plants. BMC Complement Altern Med 17: 294. https://doi.org/10.1186/s12906-017-1811-3.

Rajeshkumar S, Kumar SV, Ramaiah A, Agarwal H, Lakshmi T, Roopan SM (2018) Biosynthesis of zinc oxide nanoparticles using *Mangifera indica* leaves and evaluation of their antioxidant and cytotoxic properties in lung cancer (A549) cells. Enzyme Microb Technol 117: 91-95.

Reddy NJ, Vali DN, Rani M, Rani SS (2014) Evaluation of antioxidant, antibacterial and cytotoxic effects of green synthesized silver nanoparticles by *Piper longum* fruit. Mat Sci Engin C 34:115-22.

Salem SS, Fouda A (2020) Green Synthesis of Metallic nanoparticles and Their Prospective Biotechnological Applications: an Overview. Biol Trace Elem Res https://doi.org/10.1007/s12011-020-02138-3.

Sattari R, Khayati GR, Hoshyar R (2020) Biosynthesis of Silver–Silver Chloride Nanoparticles Using Fruit Extract of *Levisticum Officinale*: Characterization and Anticancer Activity Against MDA-MB-468 Cell Lines. J Clust Sci https://doi.org/10.1007/s10876-020-01818-3.

Siddiqui WA, Ahad A, Ahsan H (2015) The mystery of BCL2 family: Bcl-2 proteins and apoptosis: an update, Arch Toxicol 89: 289–317.

Singh J, Dutta T, Kim K, et al (2018) Green synthesis of metals and their oxide nanoparticles: applications for environmental remediation. J Nanobiotechnol 16:84.

Umar H, Kavaz D, Rizaner N (2019) Biosynthesis of zinc oxide nanoparticles using *Albizia lebbeck* stem bark, and evaluation of its antimicrobial, antioxidant, and cytotoxic activities on human breast cancer cell lines. Int J Nanomed 14:87-100.

Venugopal K, Rather H, Rajagopal K, Shanthi M, Sheriff K, Illiyas M, Rather R, Manikandan E, Uvarajan S, Bhaskar M (2017) Synthesis of silver nanoparticles (Ag NPs) for anticancer activities (MCF 7 breast and A549 lung cell lines) of the crude extract of *Syzygium aromaticum*. J Photochem Photobiol B Biol 167: 282–289.

Yu Z, Li Q, Wang J, *et al*, (2020) Reactive Oxygen Species-Related Nanoparticle Toxicity in the Biomedical Field. Nanoscale Res Lett 15: 115.

Zhelev I, Merdzhanov P, Angelova-Romova M, Zlatanov M, Antova G, Dimitrova-Dyulgerova I, Stoyanova A (2014) Lipid Composition of Carduus thoermeri Weinm., *Onopordum acanthium* L. and *Silybum marianum* L., growing in Bulgaria. Bulg J Agric Sci 20: 622–627.

Table

Table 1. Sequences of specific primers for qRT-PCR (Gholami et al. 2020).

Gene	Primer sequence
Bax	Forward: 5¢- CGGCAACTTCAACTGGGG-3′
	Reverse: 5′- TCCAGCCCAACAGCCG-3′
CAD	Forward: 5¢- TGGCAGAGATCGGAGAGCAT-3′
	Reverse: 5′- TCCTTCCATCCCTTCAGAGACTT-3′

GAPDH	Forward:	5¢ -CCCACTCCTCCACCTTTGAC-3¢
	Reverse:	5¢- CATACCAGGAAATGAGCTTGACAA-3¢

Figures

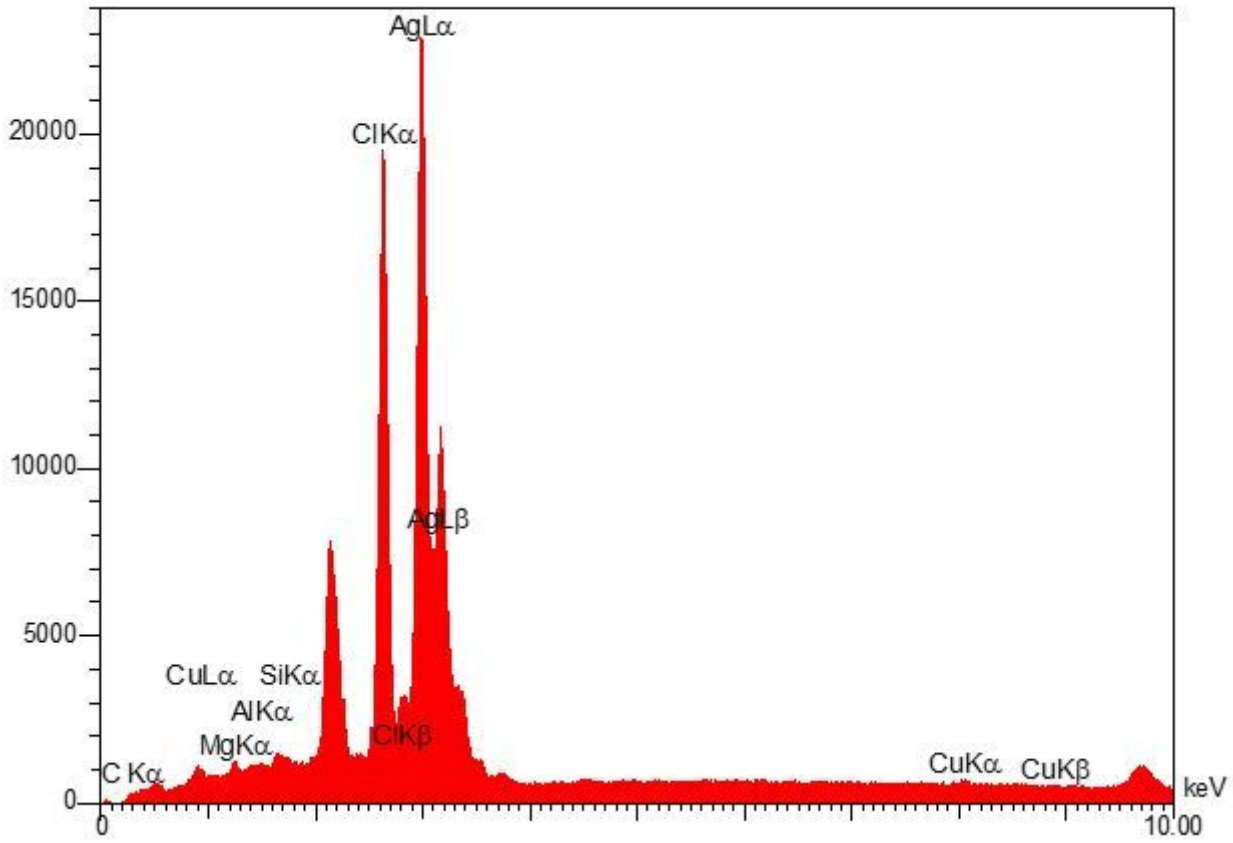

Figure 1

Energy dispersive spectroscopy (EDS) profile of fabricated AgClNPs

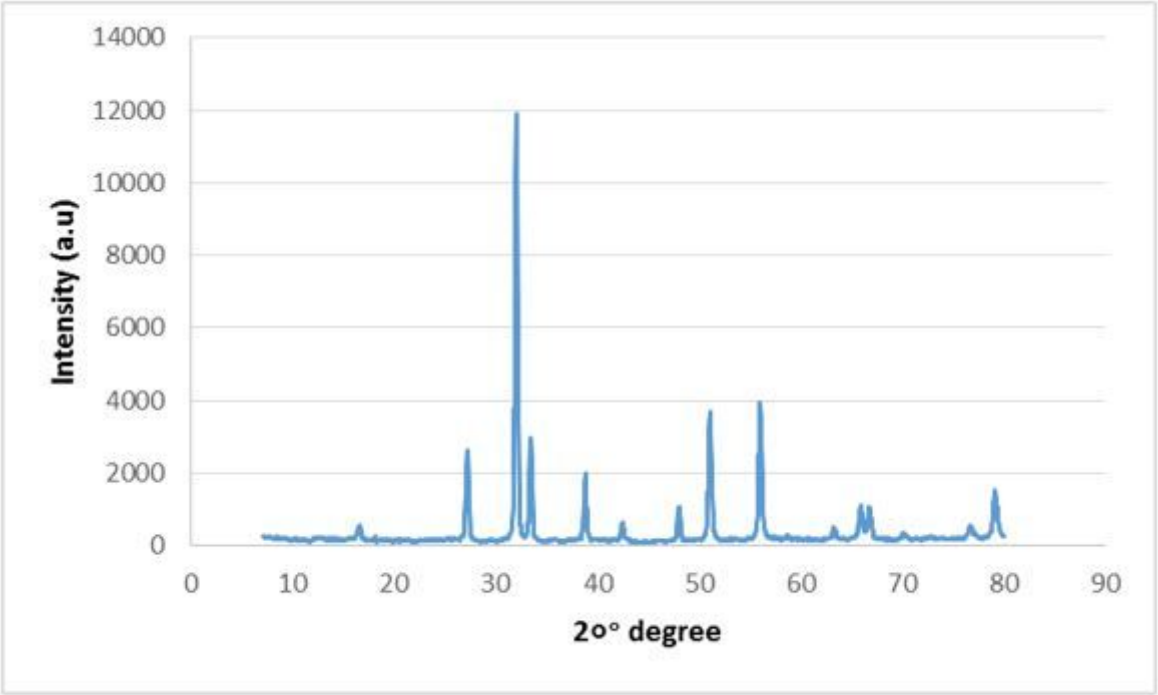

Figure 2

XRD spectrum of silver chloride nanoparticles synthesized by the dry plant Onopordum acanthium

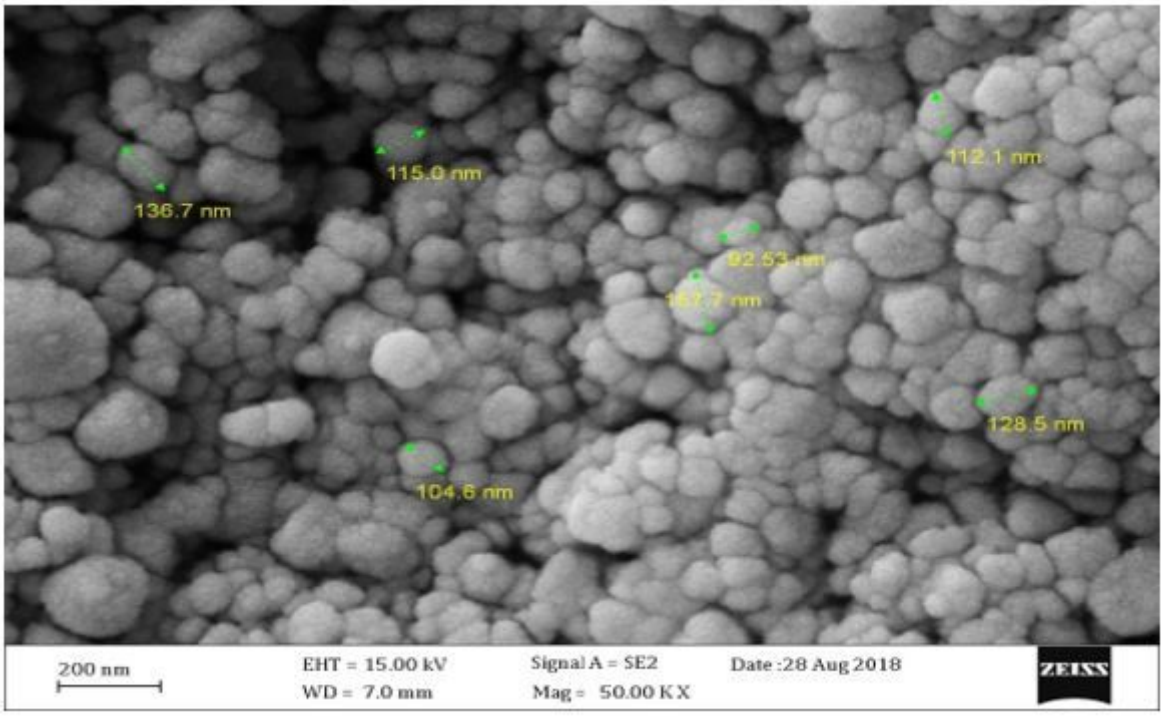

Figure 3

SEM images of silver chloride nanoparticles are made from Onopordum acanthium extract.

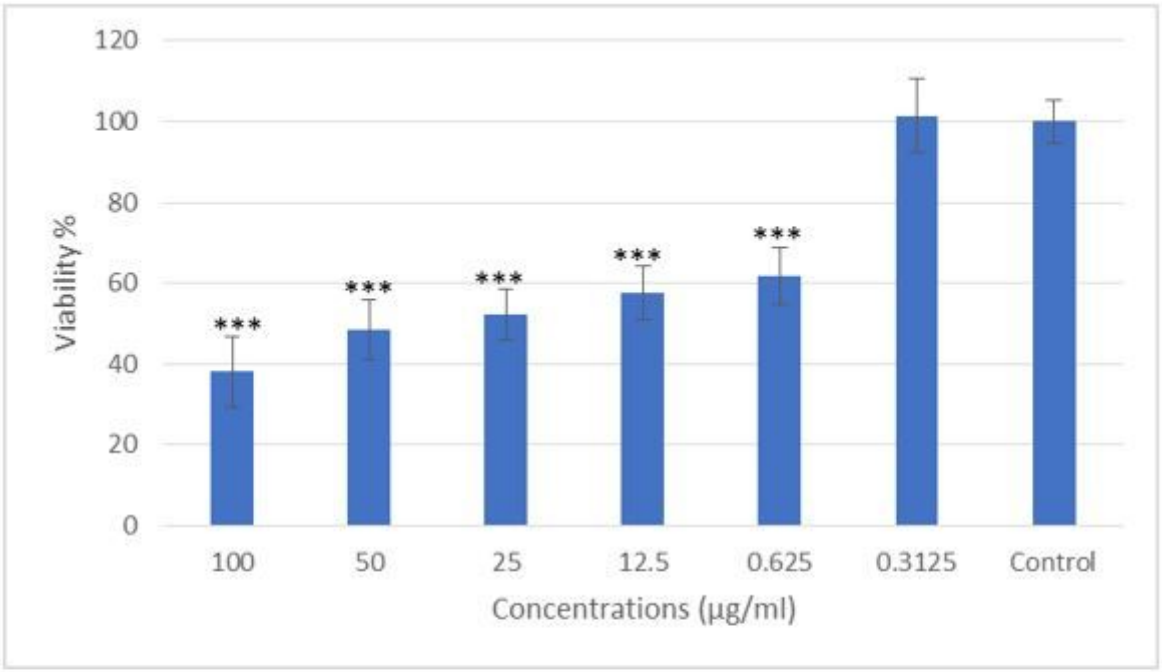

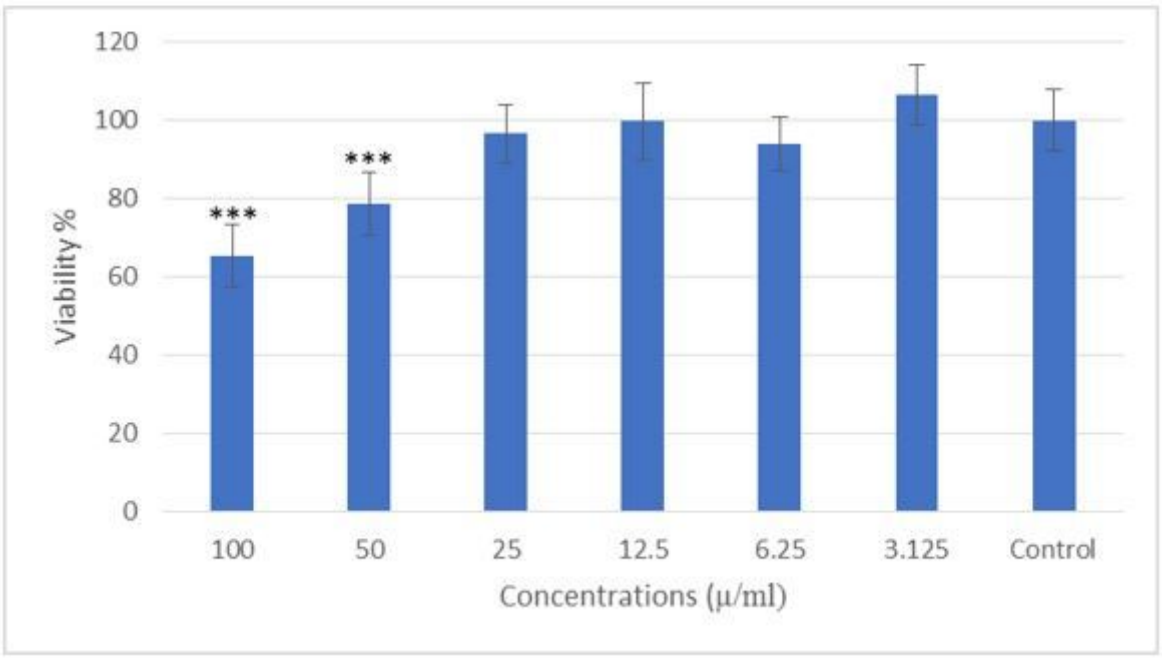

Figure 4

Measurement of cytotoxicity of MDA_MB232 (tumor cell line) (a) and HEK293 (non-tumor cell line) (b) after 24 hours of incubation with AgClNPs. Data are presented as mean ± SD. Stars (*) show a significant difference with the control group ($p < .05$, $p < .001$).

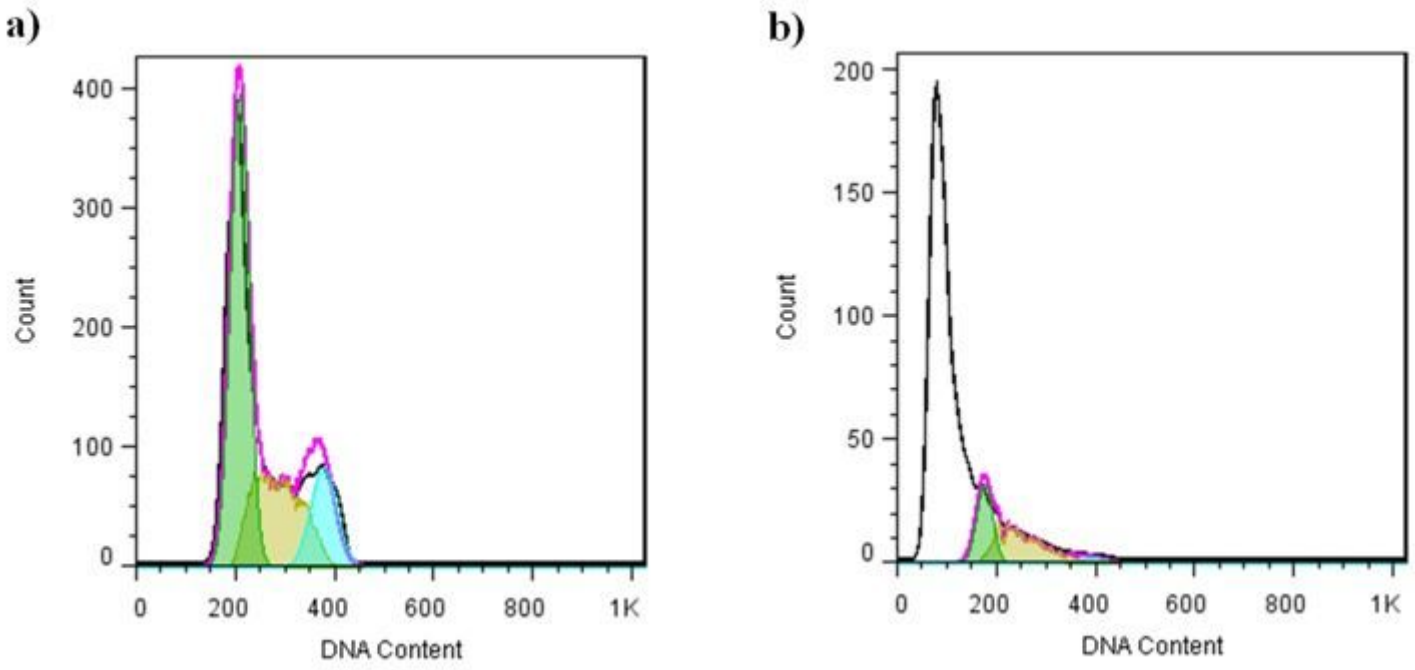

Figure 5

Effect of the fabricated AgClNPs on cell cycle phase distribution in (a) untreated and (b) treated MDA_MB232 breast cancer cells.

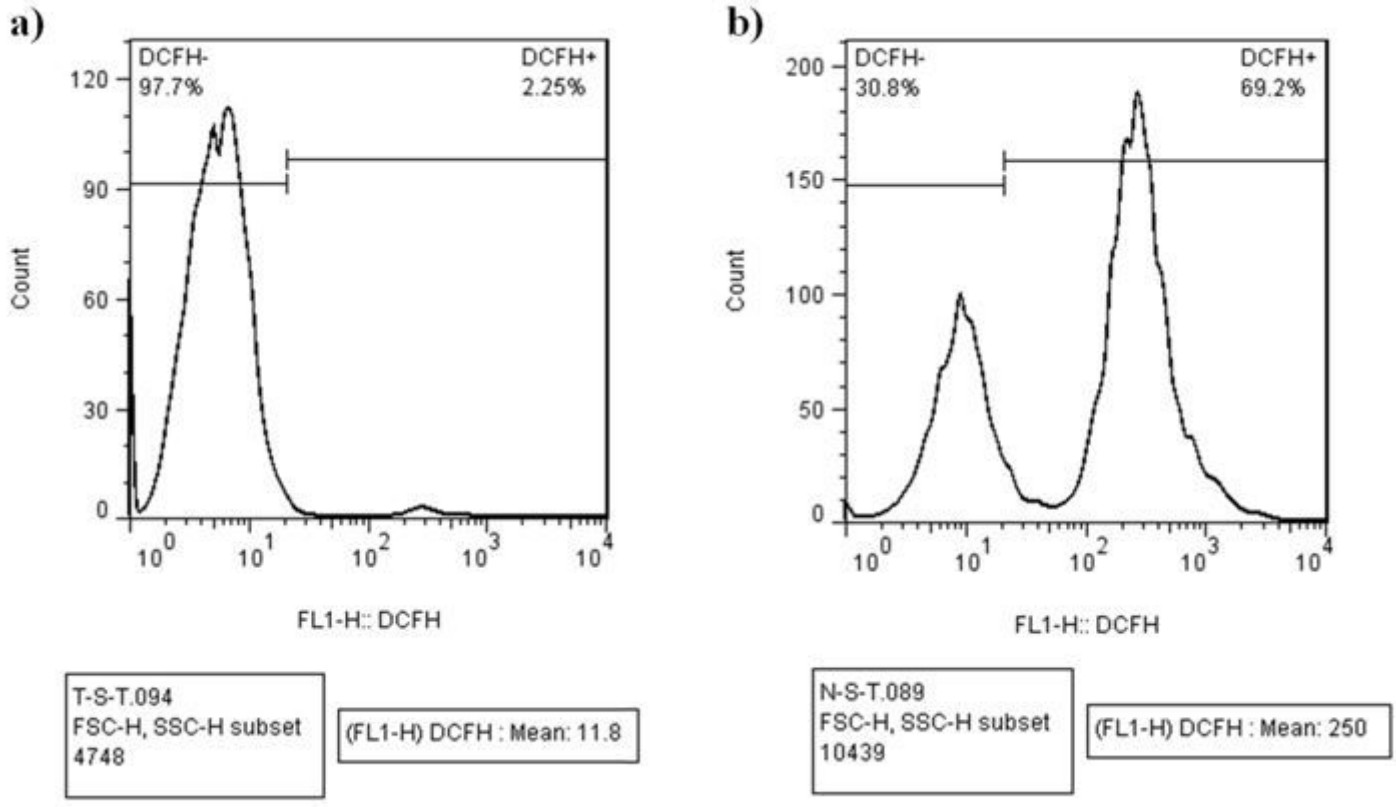

Figure 6

Effect of the fabricated AgClNPs on ROS generation in untreated (a) and treated (b) MDA_MB232 cells, followed by staining with DCFH-DA using flow cytometry.

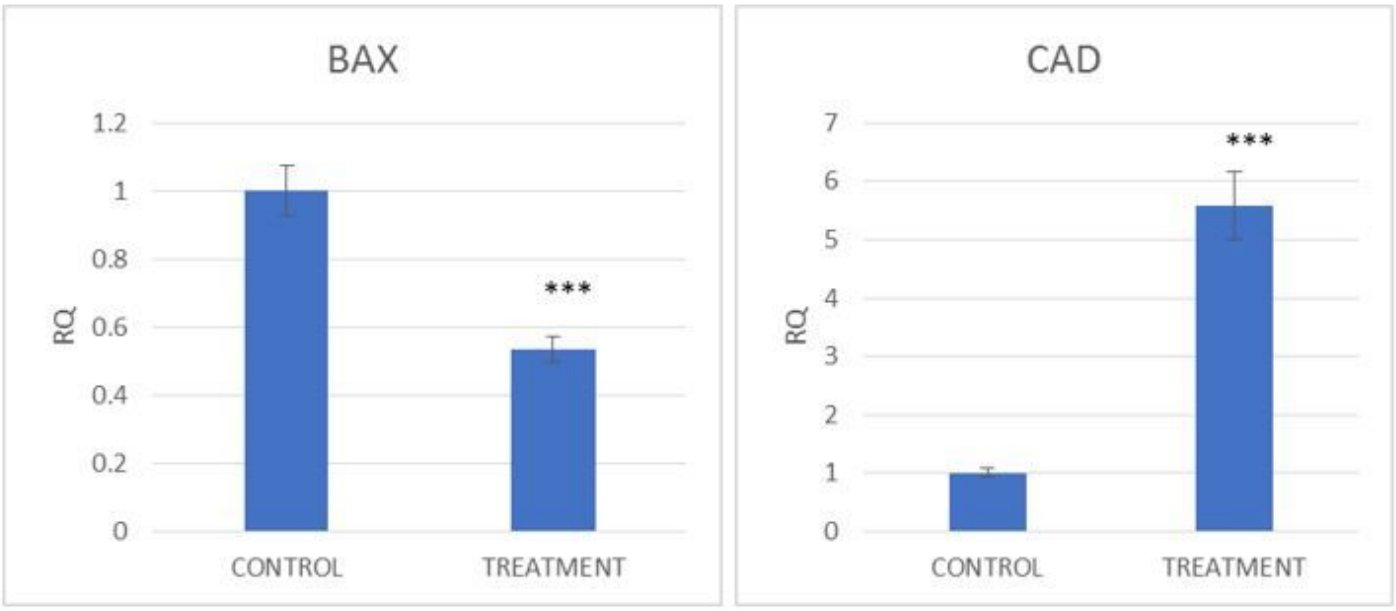

Figure 7

Transcriptional analysis of genes involved in cell death induced by moderate doses of AgClNPs after 24 h. Data are normalized to untreated cells and are reported as mean ± SD. Stars (*) show a significant difference with the control group (p <.05, p <.01, p <.001).

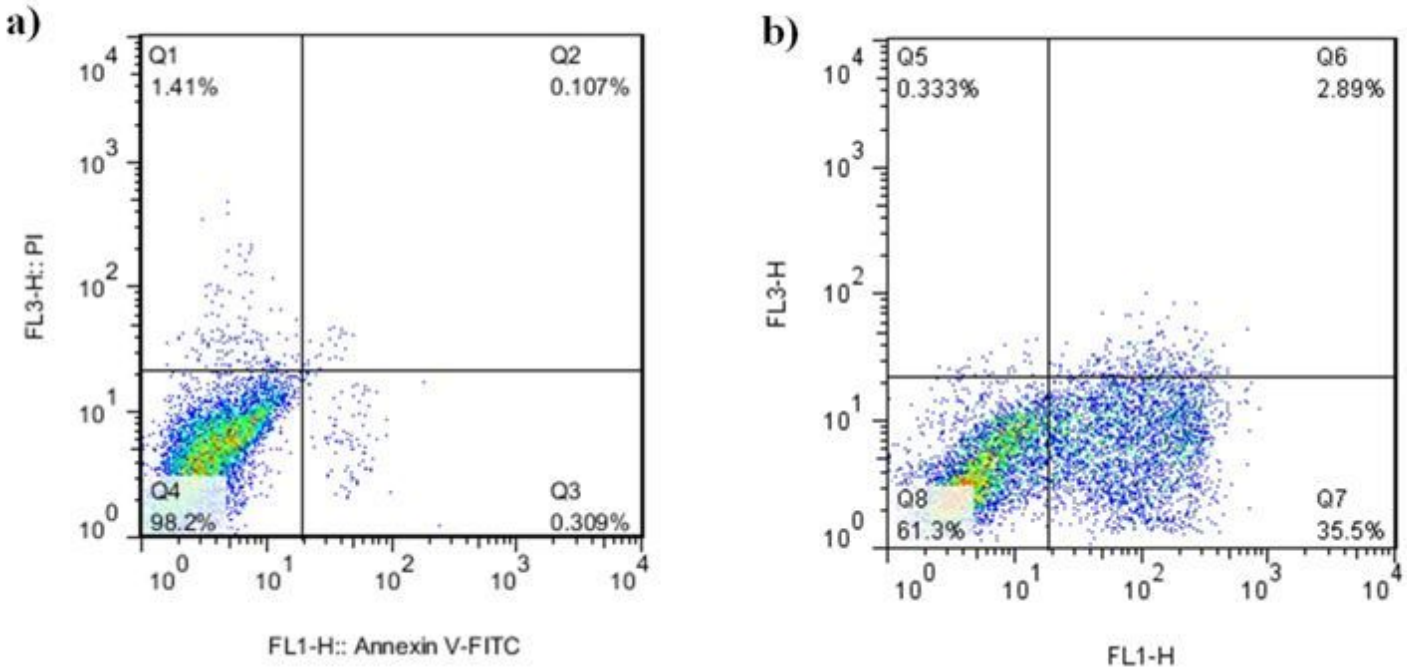

Figure 8

Annexin V/PI staining test for MDA_MB232 cells after 24 hours of incubation. Untreated control cells (a), cells treated with IC50 concentrations of synthesized AgClNPs (b) respectively.

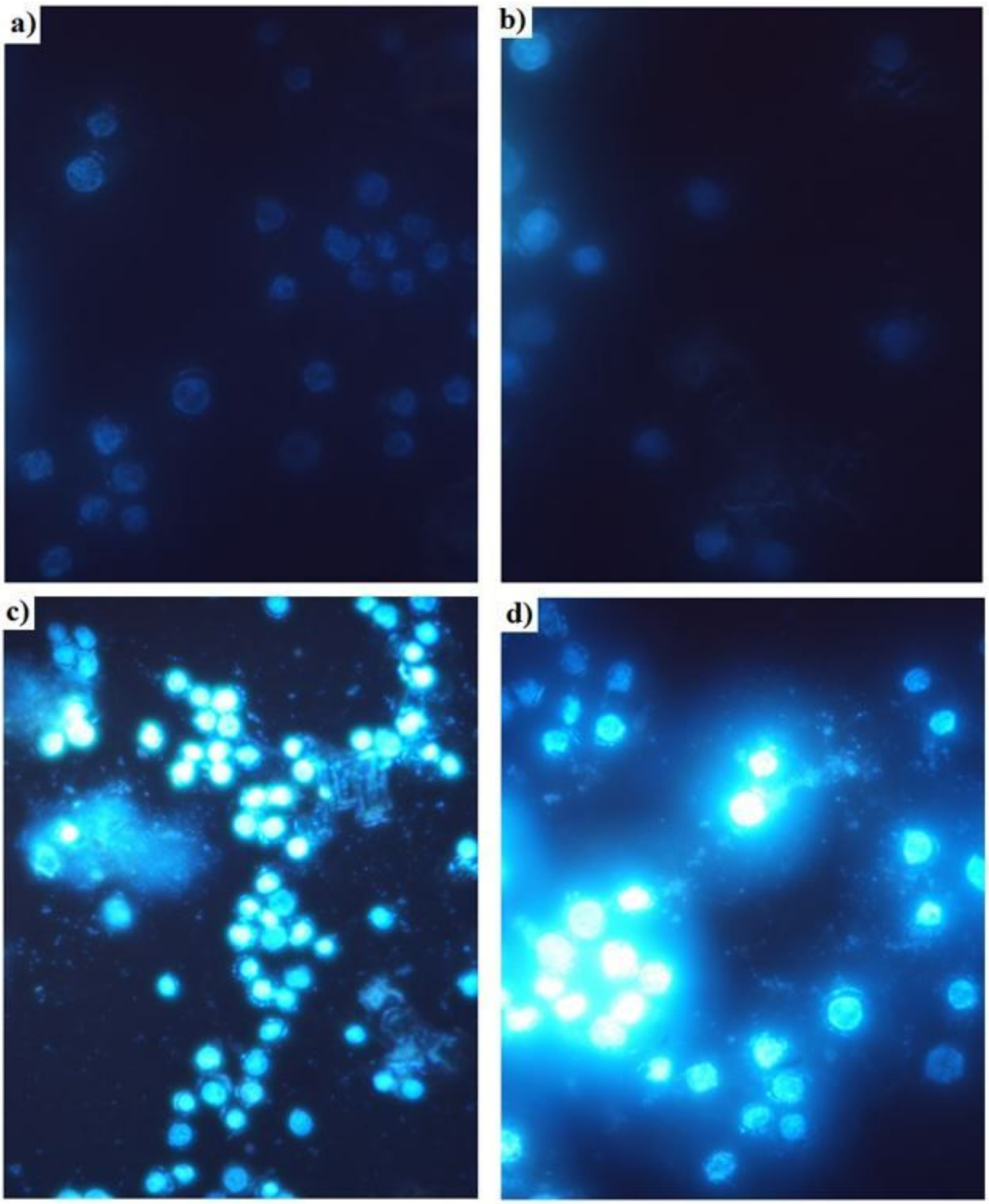

Figure 9

Morphology changes of MDA_MB232 cells with Hoescht 33258 staining under Fluorescence microscope, (a,b) Untreatment as control (b,d) exposure to IC50 concentrations of synthesized AgClNPs for 24 hours.

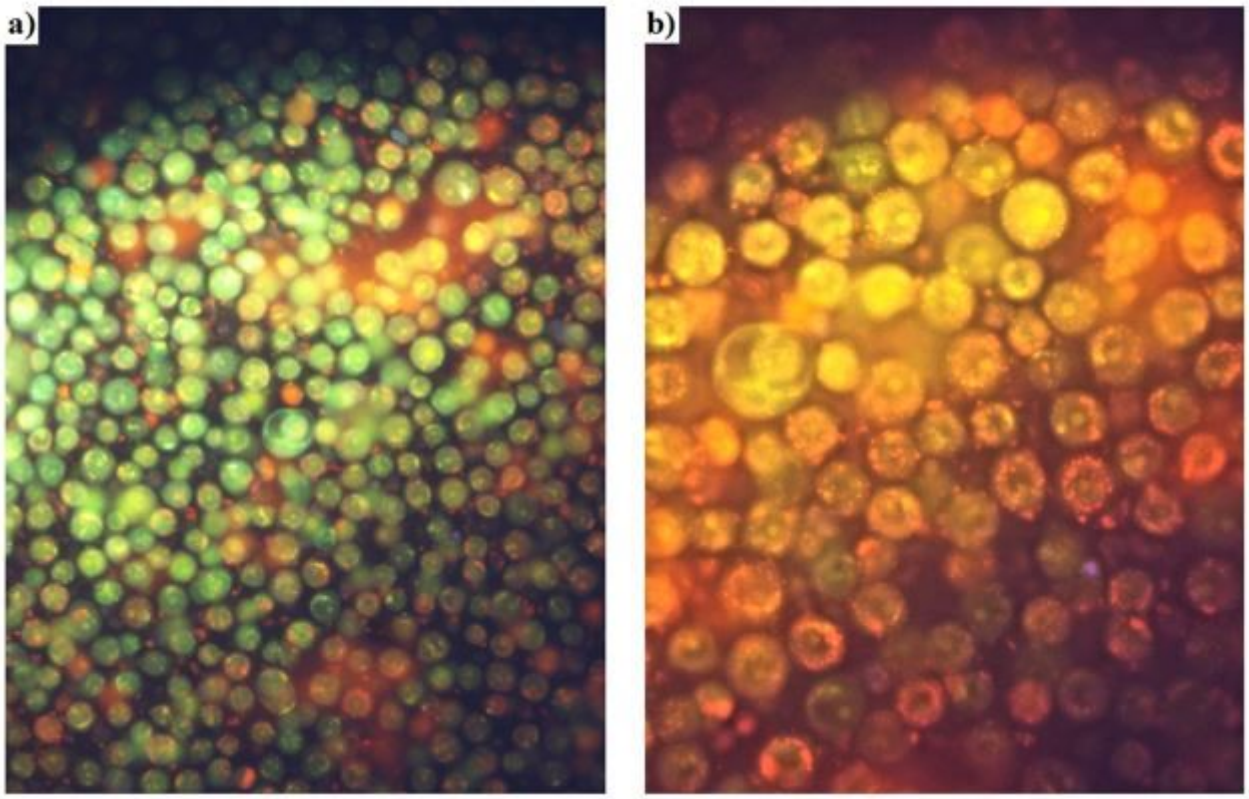

Figure 10

Fluorescence microscopic image of MDA_MB232 cells stained with AO/EB dye. Images of untreated control cells (a), AgClNPs treated with IC50 concentrations of MDA_MB232 cells (b) respectively.